

## Confined Flow in Polymer Films at Interfaces

Cynthia Buenviaje,<sup>†</sup> Shouren Ge,<sup>‡</sup> Miriam Rafailovich,<sup>‡</sup> Jonathan Sokolov,<sup>‡</sup>  
J. Mike Drake,<sup>§</sup> and René M. Overney<sup>\*,†</sup>

Department of Chemical Engineering, University of Washington, Box 351750,  
Seattle, Washington 98195-1750, Department of Materials Science, State University of New  
York at Stony Brook, Stony Brook, New York 11794-2275, and Corporate Research, Exxon  
Research and Engineering Company, 1545 Route 22 East, Annandale, New Jersey 08801

Received November 25, 1998. In Final Form: May 7, 1999

Measurements of nanomechanical properties of unannealed homopolymers show that the spin coating process in the presence of an interactive interface can be the source for molecular constraints in the interfacial boundary regime of elastomeric films. The surface mechanical response of poly(ethylene-propylene) (PEP) films of various thicknesses spin cast on hydrogen passivated silicon surfaces was studied using scanning force microscopy (SFM). At least two distinct rheological regimes can be observed in thicker films: high-entropy viscous plug flow at low load and low-entropy shear sliding at high load. The transition point from high-entropy to low-entropy shear has been found to shift to lower loads for decreasing film thickness. The transition point was found to disappear, and only shear sliding was observed at a critical film thickness, which was comparable to the radius of gyration of the sample polymer. These results were interpreted in a model wherein a highly distorted anisotropic layer induced by high-speed spinning and solvent evaporation is formed near the silicon interface. Pinning interactions prevent the layer from annealing, and a two-fluid-type response occurs. The surface free energy, determined by SFM lateral force–Dupré adhesion measurements, was found to be film thickness independent and in good agreement with previous macroscopic measurements.

### Introduction

Thin polymer films are important in many industrial applications such as protective coatings, paints, and layered polymer composites. To optimize the design and engineering of these materials, it is important to understand the interplay between confinement and molecular structure on the rheological properties. Phenomenological bulk theories, usually, neglect conformational changes on the molecular level by assuming a frame-invariant control volume. Molecular theories, on the other hand, lose track of macroscopic effects either by considering only pair interactions or assuming oversimplified mean-field or short-ranged molecular ordering. Driven by today's technological needs, it is one of the great challenges for natural sciences and engineering research to bridge the gap between phenomenological theories and molecular theories.

The mechanical properties of a polymer film depend, in a complex manner, on interfacial interactions.<sup>1–8</sup> Inter-

facial interactions determine polymer chain conformation, dynamics, and reactivity. Designing polymer films with well-defined specific shear mechanical properties and surface properties requires not only a detailed understanding of the physics but also the ability to control interfacial interaction parameters.

Concerning thin films, two interfaces have to be considered: (i) the interface at the substrate and (ii) the air–polymer interface (free surface). Recent results suggest an unchanged or increased molecular mobility at the free surface for thick films.<sup>6,9</sup> Reduced molecular mobility for ultrathin films, at the film surface, was reported on the basis of forward recoil spectroscopy measurements<sup>5</sup> and SFM.<sup>1,9</sup> In secondary ion mass spectrometry (SIMS) and SFM studies of graft copolymers, it was found that the degree of molecular ordering significantly affects dynamic processes at interfaces.<sup>1</sup> In dewetting studies of a binary homopolymer film system with negative spreading coefficients, it was found that interfacial interactions close to an interactive interface can significantly slow the molecular mobility, while a low-interaction interface does not affect the mechanical properties nor the dewetting process.<sup>1,2</sup> Self-organization of graft and block copolymers at surfaces and interfaces was studied with transmission electron microscopy (TEM) and neutron reflectivity (NR).<sup>4,10–12</sup> Pinning could be observed with surface forces apparatus studies up to a sliding velocity of about 20 nm/s

\* To whom correspondence should be addressed. Fax: 206-543-3778. E-mail: overney@cheme.washington.edu.

<sup>†</sup> University of Washington.

<sup>‡</sup> State University of New York at Stony Brook.

<sup>§</sup> Exxon Research and Engineering Co.

(1) Overney, R. M.; Guo, L.; Totsuka, H.; Rafailovich, M.; Sokolov, J.; Schwarz, S. A. *Mater. Res. Soc. Symp. Proc.* **1997**, *464*, 133–144.

(2) Overney, R. M.; Leta, D. P.; Fetters, L. J.; Liu, Y.; Rafailovich, M. H.; Sokolov, J. *J. Vac. Sci. Technol.* **1996**, *B14*, 1276–1279.

(3) Zheng, X.; Sauer, B. B.; Van Alsten, J. G.; Schwarz, S. A.; Rafailovich, M. H.; Sokolov, J.; Rubinstein, M. *Phys. Rev. Lett.* **1995**, *74*, 407–410.

(4) Zheng, X.; Rafailovich, M. H.; Sokolov, J.; Strzhemechny, Y.; Schwarz, S. A.; Sauer, B. B.; Rubinstein, M. *Phys. Rev. Lett.* **1997**, *79*, 241–244.

(5) Frank, B.; Gast, A. P.; Russel, T. P.; Brown, H. R.; Hawker, C. *Macromolecules* **1996**, *29*, 6531–6534.

(6) Liu, Y.; Russell, T. P.; Samant, M. G.; Stohr, J.; Brown, H. R.; CossyFavre, A.; Diaz, J. *Macromolecules* **1997**, *30*, 7768–7771.

(7) Liu, Y.; Rafailovich, M. H.; Sokolov, J.; Schwarz, S. A.; Zhong, X.; Eisenberg, A.; Kramer, E. J.; Sauer, B. B.; Satija, S. *Phys. Rev. Lett.* **1994**, *73*, 440–443.

(8) Tolan, M.; Vacca, G.; Wang, J.; Sinha, S. K.; Li, Z.; Rafailovich, M. H.; Sokolov, J.; Gibaud, A.; Lorenz, H.; Kotthaus, J. P. *Physica B* **1996**, *221*, 53–59.

(9) Kajiyama, T.; Tanaka, K.; Takahara, A. *Macromolecules* **1997**, *30*, 280–285.

(10) Rabeony, M.; Pfeiffer, D. G.; Behal, S. K.; Disko, M.; Dozier, W. D.; Thiyagarajan, P.; Lin, M. Y. *J. Chem. Soc., Faraday Trans.* **1995**, *91*, 2855–2861.

(11) Green, P. F.; Christensen, T. M.; Russel, T. P.; Jérôme, J. J. *J. Chem. Phys.* **1990**, *92*, 1478–1482.

(12) Russel, T. P.; Menelle, A.; Anastasiadis, S. H.; Satija, S. K.; Majkrzak, C. F. *Macromolecules* **1991**, *24*, 6263–6269.

(or a transit time larger than 0.025 s).<sup>13</sup> The authors concluded that (i) the nonpinning regime is due to the vibrations of the molecular groups which define a potential energy valley at the interface and (ii) in a highly compressed polymer film at low lateral shear velocities shear alignment occurs on the molecular scale.<sup>13</sup>

Recently, we have used a series of complementary techniques (SFM,<sup>1</sup> SIMS,<sup>1</sup> and NR<sup>4</sup>) to determine the range of the interactions due to attractive interfaces. We found strong deviations from the bulk in the tracer diffusion coefficients, the local viscosity, and the mechanical properties at distances over 200 nm from the substrate which in some cases corresponded to more than 10 times the bulk polymer radius of gyration,  $R_g$ .<sup>1,4</sup> It is fairly easy to understand the change in mechanical properties and mobility for film thicknesses on the order of  $2R_g$ , where almost every chain has at least one contact with the surface. On the other hand, the persistence of the effect at distances much larger than  $R_g$ , where almost none of the chains are in direct contact with the surface, is far more difficult to explain. Existing classical mean field or molecular dynamic theories assume that the surface interaction is completely screened within a distance corresponding to the persistence length of the polymer (about 0.6 nm).<sup>14,15</sup> This assumption may not be completely valid in the case of spin casted films where the solvent evaporation leaves voids, and hence, excluded volume and compressibility have to be considered. In spin casted films the situation is even more complex. It is well-known that polymers in solution are less entangled than those in the melt. Sauer et al. have shown that, in the spin casting process, the solvent can evaporate faster than the relaxation time of the chains.<sup>16</sup> Hence, the lower entanglement density may be temporarily preserved if the films are held below the glass transition temperature of the polymer. Since Zheng et al. have shown that surface pinning can drastically reduce the mobility of polymers near surfaces,<sup>4</sup> effects of an interactive surface on the ability of a polymer film to relax have to be considered even above the glass transition temperature.

In this paper, we explore the surface mechanical properties as a function of thickness for spin casted and temperature unannealed films using lateral scanning force microscopy. We will present possible explanations concerning the origin of the long-range effect of the previously described interfacial confinement. We will provide a model of the interfacially confined boundary layer and compare the strain imposed onto the polymer matrix by the spin coating process with the strain induced during molecular shear alignment at the surface.

## Experimental Section

Polymer films, of varying thickness between 20 and 520 nm, were made by spin casting monodispersed ( $M_w = 374\,000$ ,  $M_w/M_n < 1.1$ ) poly(ethylene-co-propylene) (PEP,  $T_g = -62\text{ }^\circ\text{C}$ )<sup>17</sup> from toluene solution onto HF etched (hydrogen passivated)<sup>18</sup> silicon wafer. The bulk radius of gyration  $R_g$  of the polymers was determined to be 24.3 nm. Film thicknesses were determined by ellipsometry (autoEl, Rudolph). The films were dried for ap-

proximately 1 week at room temperature under atmospheric pressure and intentionally left unannealed prior to scanning.

A commercial atomic force microscope (Explorer from Thermomicroscopes), which is based on a laser beam deflection detection scheme, was used in conjunction with a digital oscilloscope (54601B from Hewlett-Packard) for lateral force (friction) measurements. Triangular silicon nitride cantilevers (Model 1530 from Thermomicroscopes) were used. The lateral force,  $F_L$ , was calibrated using the following relationship:<sup>19</sup>

$$F_L = \Gamma I_T; \quad \Gamma = \mu_{\text{cal}}(\Delta I_T^{\text{cal}}/\Delta F_N^{\text{cal}})^{-1} \quad (1)$$

where  $\mu_{\text{cal}} = 0.18 \pm 0.03$  was determined from a silicon calibration sample with a bar shaped cantilever,  $\Gamma$  is the calibration geometry factor which is determined by the blind-calibration method described in ref 19,  $S$  is the sensitivity of the photodiode determined from the slope in the force-displacement curve, and  $I_T$  is the signal of the photodiode;  $S$  and  $I_T$  are induced by the normal and torsional deflection of the cantilever, respectively, obtained during sliding on the sample surface. The index "cal" refers to signals obtained from the silicon calibration sample. The calibration geometry factor,  $\Gamma$ , was determined to be 5.3 with a normal spring constant  $k_N$ , of 0.064 N/m. Cut silicon wafers (100) (Silicon Sense Inc.) were used as lateral force calibration standards (for details see ref 19).

The resistance of sliding was measured as a function of the normal force at a scan rate of 0.5 Hz over a distance of 20  $\mu\text{m}$ . The net contact force,  $F_N$ , corresponds to the applied load only when it is positive. Negative values are due to adhesion forces. Based on contact mechanics for nonconforming axisymmetric solids, the cantilever jump-off instability is reached, when

$$F_N = -F_{\text{adh}} = -3\pi R\gamma \quad (2)$$

where  $F_{\text{adh}}$  is the instability force of adhesion,  $\gamma$  is the work of adhesion per unit area, and  $R$  is the radius of curvature of the cantilever tip.<sup>20</sup> The adhesion instability forces were determined by force displacement measurements.

## Results and Discussion

**Shear Behavior of Thick Bulklike Films.** Friction measurements on a monodisperse PEP film of 520 nm thick, Figure 1, show three distinct friction-load regimes: (i) In a low-load regime,  $F_N < 12.5$  nN, the friction force has a parabolic relationship with the applied load. (ii) In an intermediate load regime,  $12.5 < F_N < 33$  nN, the friction force varies linearly with the applied load. (iii) In a large force regime,  $F_N > 33$  nN, the friction force varies slowly with load with a significantly decreased friction coefficient compared to the intermediate load regime.

In the case of a very soft sample, the loads belonging to the approach and retraction instabilities are comparable. Only for stiffer surfaces and/or lower interaction forces, the load can be reduced by pulling the cantilever back toward the jump-off (retraction) instability (see details in ref 19). A convex shaped parabolic friction-load relationship is evidence for plastic indentation of a sphere-plane geometry.<sup>21</sup> Considering the liquidlike nature of the samples, we can assume that the indentation is fully plastic. The cantilever-shape-induced parabolic behavior of the friction-load function has been discussed by Pittenger et al. who modeled the cantilever tip as a cone truncated with a portion of a hemisphere.<sup>21</sup> Following this model, we can assume that below 12.5 nN the contact is provided by the hemisphere.

(13) Georges, J.-M.; Tonck, A.; Loubet, J.-L.; Mazuyer, D.; Georges, E.; Sidoroff, F. *J. Phys. II* **1996**, *6*, 57–76.

(14) de Gennes, P. G. *Scaling Concepts in Polymer Physics*; Cornell University Press: Ithaca, NY, 1979.

(15) Brogley, M.; Bistac, S.; Schultz, J. *Macromol. Theor. Simul.* **1998**, *7*, 65–68.

(16) Sauer, B. B.; Walsh, D. J. *Macromolecules* **1994**, *27*, 432–440.

(17) Cheremisinoff, N. P. *J. Macromol. Sci. Chem.* **1989**, *A26*, 1231–1259.

(18) Higashi, G. S.; Chabal, Y. J.; Trucks, G. W.; Raghavachari, K. *Appl. Phys. Lett.* **1990**, *56*, 656–658.

(19) Buenviaje, C.; Drake, J. M.; Pictrosky, C. F.; Overney, R. M. To be submitted for publication.

(20) Johnson, K. L. *Contact Mechanics*; Cambridge University Press: Cambridge, U.K., 1987.

(21) Pittenger, B.; Cook, D. J.; Slaughterbeck, C. R.; Fain, S. C. *J. Vac. Sci. Technol. A* **1998**, *16*, 1832–1837.

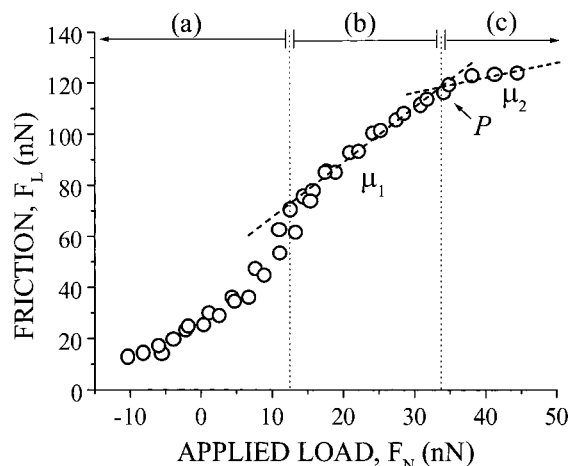


**Figure 1.** Friction vs load dependence on a 520 nm thick PEP film using a silicon nitride tip. Three regimes can be differentiated in the friction–load relationship. (i) Up to a load of 12.5 nN the friction–load function is parabolic due to the spherical shape of the very end of the cantilever tip; (ii) between 12.5 and 33 nN viscous plug flow occurs with a strongly loading dependent contact area which leads to a high friction coefficient of 2.1; (iii) above 33 nN the PEP surface is strain hardened (disentangled stretched polymer chains) with a less loading dependent contact area, and hence, low friction coefficient of 0.3. The point  $P$  denotes the transition point.

For loads higher than 12.5 nN, the indentation is governed by the shaft of the cone. That causes the contact area to change linearly with load, as it is observed in the intermediate force regime shown in Figure 1 where a linear friction–load relationship is obtained. A friction coefficient,  $\mu_1 = 2.09$ , can be deduced from the slope of the curve. At such high friction coefficients sliding cannot occur without plastic deformation.<sup>20</sup> It is well-known from contact mechanics that the maximum pressure is concentrated below the sample surface.<sup>20</sup> Thus, the cantilever sliding process causes viscous plug flow in the liquidlike polymer system.

The Young's modulus of the film can be obtained from the tangential traction for a sphere–plane contact given by the Hertz theory and Amontons' law of friction:<sup>20</sup>

$$q(r) = \mu p(r) = \frac{3\mu F_N}{2\pi a^3} [a^2 - r^2]^{1/2} \quad (3a)$$

$$p(r=0) = \frac{3F_N}{2\pi a^2} = \left( \frac{6F_N E^2}{\pi^3 R^2} \right)^{1/3} \quad (3b)$$

where  $q(r)$  and  $p(r)$  are the distributions of traction and pressure, respectively, and  $\pi a^2$  is the contact area. The Young's modulus,  $E$ , can be determined, if the contact radius,  $a$ , and the radius of curvature,  $R$ , are known. On the basis of the resolution limit at steps of  $\text{CaF}_2$ , we assume a 10 nm curvature of the cantilever tip, which is in correspondence with our adhesion measurements (see below). It is reasonable to assume that the maximum contact radius of the spherical hemisphere is reached for an applied load of 12.5 nN. Hence the assumed curvature of the tip, 10 nm, corresponds to the radius of maximum contact at a load of 12.5 nN which leads to a contact area of 314 nm<sup>2</sup>. Substituting these values into eq 3, we obtain a Young's modulus that is in good agreement with the bulk value in the literature of 15 MPa.<sup>22</sup> Note that pressures of that magnitude are close to yield pressures

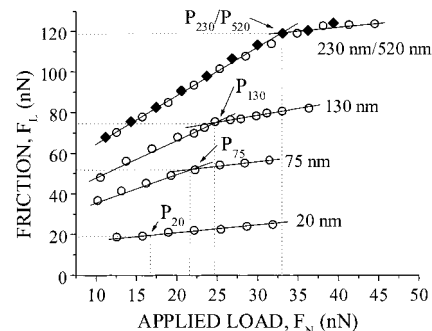


**Figure 2.** Film thickness in the intermediate to high loading regime. Viscous flow–sliding transitions,  $P_x$  ( $x = 75, 130, 230, 520$  nm) are found for films thicker than 20 nm. The transition point,  $P_{20}$ , has been extrapolated from Figures 3 and 4.

in polymeric systems. Hence, our assumption of a plastic deformation in the intermediate- to high-load regime is justified.

The transition between the intermediate- and high-load regimes can be defined by the intercept,  $P$ , shown in Figure 1. Above a load of  $F_N = 35$  nN, the friction coefficient is found to decrease significantly (Figure 1). At the intercept,  $P$ , three-dimensional viscous shear is replaced by a two-dimensional sliding process. This transition point is the surface or interfacial analogue to a phase transition in the polymer. For lower loads the polymer, which is a viscous fluid at room temperature, exerts a drag force on the moving tip and undergoes plug flow. As the load is increased, the tip plows deeper into the liquid and the drag increases with increasing flow. In addition to viscous drag, some of the frictional energy is also dissipated in stretching the polymer chains. At point  $P$ , a crossover occurs where most of the additional shear energy is now dissipated in chain stretching as opposed to penetrating deeper into the sample. Above point  $P$ , the shear process is basically occurring two-dimensionally. This leads to the analogue of a phase transition of decreased entropy. Further increase in load will eventually lead to chain scission and removal of the film from the substrate. Topographic images of the film surface over an expanded region do not show any visible damage since the polymer film is above  $T_g$  and can flow to anneal the furrows induced by the tip. Hence, no permanent damage results.

**Shear Behavior of Thin Films.** The friction force behavior as a function of loading is shown in Figure 2 for PEP films of different thickness,  $t$ , ranging from 20 to 520 nm. Only the sample specific intermediate- and high-loading regimes are shown. Two trends become apparent: First, for films with  $t < 200$  nm, the overall frictional force decreases rapidly with the film thickness. This effect is very surprising since the film is at least 8–10  $R_g$  thick at the onset. Second, the plug flow regime (i.e., the intermediate friction regime) becomes smaller and finally disappears completely for films of  $t = 20$  nm (approximately  $R_g$ ). This is illustrated in Figure 3, where we plot the transition point,  $P$ , derived from Figure 2, as a function of film thickness. The intercept point  $P$  is found to shift to lower normal loads for thin PEP films. At a film thickness larger than 230 nm the measured transition friction force corresponding to  $P$  is 120 nN. At a film thickness of 75 nm, the transition friction value is 52 nN. If we extrapolate from the data obtained for thicker films, Figure 3, we find that the transition point,  $P$ , for the thinnest film studied (20 nm) should occur at a load of 19 nN which is well within the experimental range studied. Yet, it is interesting to note that no transition point is observed for the 20 nm thick PEP film.

(22) Gotro, J. T.; Graessley, W. W. *Macromolecules* **1984**, *17*, 2767–2775.

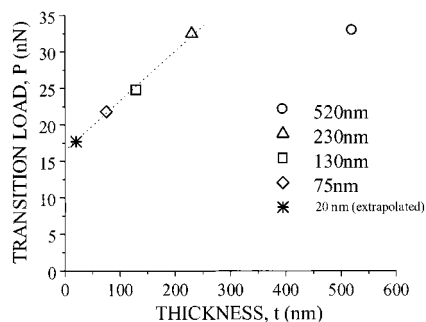


**Figure 3.** Transition load,  $P$ , as a function of PEP thickness. At the transition load, the lateral strain in the polymer structure is maximum. Less load is necessary in very thin films to reach the maximum strain. Above 200 nm thickness the films are initially in the unstrained bulk phase.

In previous studies on PEP and polystyrene (PS) films annealed above their respective  $T_g$ , we found that the properties of the films change in the vicinity of interactive substrate such as silicon.<sup>1</sup> For PS, the tracer diffusion coefficients, which are inversely proportional to the zero shear viscosity, were found to gradually decrease by more than 2 orders of magnitude with decreasing film thickness.<sup>4</sup> Simple surface pinning was ruled out since the onset of the effect appeared at approximately 200 nm, or at least 10  $R_g$  distance from the interface where the probability of direct surface contact was nearly zero. A similar effect was observed for PEP in dewetting experiments where the velocity of the dewetting film was inversely proportional to the viscosity.<sup>1</sup> Surface mechanical measurements of PEP films showed a similar trend.<sup>1</sup> As the film thickness decreased from approximately 200 nm, the film surface became more elastic and less viscous, approaching the characteristics of a completely solid surface for films of 200 nm. The present rheological data are consistent with these findings and provide an explanation for the long-range effects of the interactive surface. For films thicker than 200 nm, the polymer is able to flow freely and the buried interface is not felt. As the films become thinner, free plug flow is now impeded by the confining interface and the transition point occurs earlier. Finally for films around  $R_g$ , interactions with the surface make all flow impossible, the material becomes "solidlike", and no transition point is observed because shear sliding occurs at any load at the interface.

High-resolution X-ray reflectivity data were obtained at the Cu wavelength and showed a decreasing density of 10% for thin films (40 nm) prior to annealing compared to thick films (500 nm).<sup>23</sup> The density defect disappeared upon annealing in agreement with recently published neutron reflectivity measurements.<sup>24</sup> A decreasing density was observed by X-ray reflection on the 20 nm thick PEP film compared to thick films.

**Surface and Interfacial Energies of Strained and Unstrained Films.** The functional relationship between the jump-off adhesion force,  $F_{adh}$ , and the transition load,  $P$ , at the transition point,  $P$ , is illustrated in Figure 4 for  $t = 75\text{--}520$  nm. The linear relationship signifies that the plug flow-sliding transition occurs independent of the film thickness at a constant transition pressure. Considering the functional relationship of the transition load with the film thickness, Figure 3, it can also be concluded that the contact area is varying with the film thickness. Because the transition load is increasing with increasing

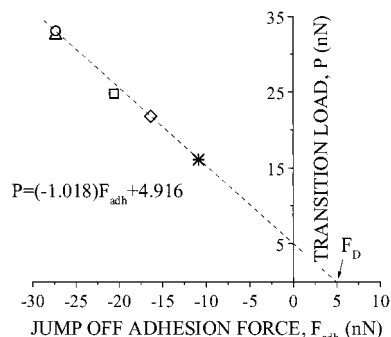


**Figure 4.** Functional relationship between the jump-off adhesion force,  $F_{adh}$ , and the transition load,  $P$ , for 75–520 nm film thickness. The intercept of the axis of the adhesion force, the Dupré adhesion force  $F_D$ , is 5 nN. The slope is  $-1.0$ .

film thickness, the contact area has to decrease with film thickness so that the transition pressure remains constant. This is in correspondence with the X-ray density measurements documenting a decrease in density for a decrease in film thickness.<sup>23</sup> In addition, we found that the surface roughness is decreasing with increasing film thickness.

A negative slope of about 1 and an adhesive force intercept, the Dupré adhesion force  $F_D$ , of 5 nN are found in Figure 4. The corresponding Dupré's work of adhesion (per unit area of contact) is defined as

$$\gamma_D = \gamma_1 + \gamma_2 - W_{12}; \quad W_{12} = 2\gamma_{12} \quad (4)$$

where  $\gamma_1$  and  $\gamma_2$  are the free surface energies of the two bodies,  $\gamma_{12}$  is the interfacial energy per unit area, and  $W_{12}$  represents the work of adhesion required to separate two solid surfaces, excluding any energy of deformation.<sup>25–27</sup> It is important to note that the instability adhesion or "jump-off" adhesion,  $F_{adh}$ , alone is insufficient for a discussion of load-independent interfacial interactions because  $F_{adh}$  is a convoluted result from interfacial interactions and contact deformations (more detailed discussions can be found in refs 19, 21, 26, and 27).

The JKR theory<sup>28,29</sup> connects the "pull-off" adhesion force with the work of adhesion by  $F_{adh}(P_{max}) = 3\pi R\gamma(P_{max})$ , assuming a sphere–plane contact at the maximum applied force,  $P_{max}$ , during an adhesion measurement.  $P_{max}$  is important as it takes strain into account. The load,  $P$ , corresponding to the transition point,  $P$ , fulfills the criteria of a maximum load because no further strain occurs at higher load (see discussion above). Hence the load-independent work of adhesion (per unit contact area),  $\gamma_D$ , is given by

$$\gamma_D = \frac{1}{3\pi R} \lim_{P_{max} \rightarrow 0} F_{adh}(P_{max}) = F_D/3\pi R \quad (5)$$

$\gamma_D$  is calculated to be 53 dyn/cm for a radius of curvature of 10 nm (see above) and a Dupré adhesion force of 5 nN. This is in excellent agreement with the following set of interfacial and surface energies:  $\gamma_{Si-nitride} = 92$  dyn/cm,  $\gamma_{PEP} = 30.9$  dyn/cm,<sup>2</sup> and  $\gamma_{12} = 35$  dyn/cm. Only dispersion forces were considered for the interfacial tension; i.e.,  $\gamma_{12}$

(25) Israelachvili, J. *Intermolecular & Surface Forces*; Academic Press Inc.: London, 1991.

(26) Pollock, H. M.; Maugis, D.; Barquins, M. *App. Phys. Lett.* **1978**, *33*, 798–799.

(27) Maugis, D.; Pollock, H. M. *Acta Metall.* **1984**, *32*, 1323–1334.

(28) Johnson, K. L.; Kendall, K.; Roberts, A. D. *Proc. R. Soc. A* **1971**, *324*, 301–313.

(29) Greenwood, J. A. *Proc. R. Soc. London A* **1997**, *453*, 1277–1297.

(23) Wu, L. W. To be submitted for publication.

(24) Wallace, W. E.; Tan, N. C. B.; Wu, W. L. *J. Chem. Phys.* **1998**, *108*, 3798–3804.

$= [\gamma_{\text{PEP}}^d \gamma_{\text{Si}}^d]^{1/2}$ ,<sup>30</sup> with  $\gamma_{\text{PEP}}^d = 30.0 \text{ dyn/cm}^2$  and  $\gamma_{\text{Si}}^d = 40 \text{ dyn/cm}$  (the surface tension of the silicon–nitride surface is reasonably well approximated by a silicon–oxide surface).<sup>16</sup>

Note that surface and interfacial energies were not found to depend on the amount the films are strained.

### Conclusion and Summary

The spin casting process induces a strain in the polymer films which is frozen in as the solvent is rapidly evaporated. Since the glass transition of PEP is well below room temperature, annealing and relaxation of the chains occurs under ambient conditions. Voids which are left behind by the solvent are removed, and the melt density is recovered. On the basis of the above presented surface mechanical data obtained from unannealed ultrathin PEP films, and previous studies of thin annealed PEP<sup>1</sup> and annealed and unannealed PS<sup>4</sup> films, we suggest the following structural model:

(i) The layer immediately adjacent to the silicon substrate (*sublayer*) is pinned to the surface. As a result this layer cannot be relaxed even above the  $T_g$  of the polymer. The dynamics of this layer are determined mainly by the nature of the pinning interaction. Since the  $T_g = -62 \text{ }^\circ\text{C}$  of PEP is far below room temperature, the chains that are not immediately pinned to the surface are mobile and can relax by diffusing into the less entangled network<sup>16</sup> of the sublayer. The strained interfacial sublayer can be pictured as highly disentangled and laterally anisotropic with a thickness on the order of the polymer's radius of gyration.

(ii) The polymers adjacent to the surface immobilized sublayer can diffuse through the sublayer's pores, forming a two-fluid system, as previously observed in a PS system.<sup>4</sup> A boundary layer is formed between the interfacial sublayer and the polymer bulk phase which is structurally and mechanically different from the bulk. The boundary layer thickness for PEP is found to extend over a distance of  $7\text{--}10 R_g$ . Similar far-field effects were found also in PS systems.<sup>4</sup> SFM strain experiments let us conclude that

the polymers are less entangled in the boundary layer than in the interfacial sublayer, and gradually reach the entanglement of the polymer melt for an increasing distance from the substrate. It is important to note that the normal diffusion into the pores of the interfacial sublayer causes an additional anisotropy in the boundary layer in normal direction. We believe that it is this normal anisotropic component paired with film properties (e.g., molecular weight) and spin casting conditions which are responsible for the observed far-field effects of interfacial confinement.

(iii) Finally, at a distance of about  $7\text{--}10 R_g$  apart from the substrate, the polymer behaves like the bulk elastomer and loses any memory of the presence of the silicon surface and the spin-coated induced interfacial alignment.

Flow and sliding properties of different thickness regions have been studied by SFM. In thick films, the flow is unhindered and classical plug flow occurs. A rapid increase in friction with load is observed as expected if the contact area (and with it the jump-off adhesion) is loading dependent. A surface transition point from three-dimensional viscous flow to two-dimensional interfacial sliding is observed at high pressure. This transition could illustratively be presented as the "barrier height for disentanglement" which would be the phase transition analogue from a melt to a gel. The thinner the film (or the closer the material is probed to the sublayer), the faster the transition to a gellike material occurs, as the flow is hindered by the altered mechanical and structural properties in the boundary layer. Finally, when the film thickness is comparable to the immobilized sublayer, no flow occurs, only sliding. Hence, the interfacial sublayer is already in a gellike state.

**Acknowledgment.** This project was made possible through the financial support of the Exxon Educational Foundation and the Royalty Research Fund (University of Washington). Partial support from NSF MRSEC (Grant DMR96325235) on different aspects of this work is gratefully acknowledged. We wish to thank Wen Li Wu for sharing with us his X-ray reflection data.

LA9816499

(30) Adamson, A. W. *Physical Chemistry of Surfaces*, 3rd ed.; Wiley: New York and London, 1976.